A LETTERS JOURNAL EXPLORING THE FRONTIERS OF PHYSICS

OFFPRINT

Dual landscapes in Anderson localization on discrete lattices

M. L. LYRA, S. MAYBORODA and M. FILOCHE

EPL, **109** (2015) 47001

OVER
560,000
full text downloads in 2013

24 DAYS
average accept to online publication in 2013

10,755
citations in 2013

"We greatly appreciate the efficient, professional and rapid processing of our paper by your team."

Cong Lin
Shanghai University

Six good reasons to publish with EPL

We want to work with you to gain recognition for your research through worldwide visibility and high citations. As an EPL author, you will benefit from:

1. **Quality** – The 50+ Co-editors, who are experts in their field, oversee the entire peer-review process, from selection of the referees to making all final acceptance decisions.
2. **Convenience** – Easy to access compilations of recent articles in specific narrow fields available on the website.
3. **Speed of processing** – We aim to provide you with a quick and efficient service; the median time from submission to online publication is under 100 days.
4. **High visibility** – Strong promotion and visibility through material available at over 300 events annually, distributed via e-mail, and targeted mailshot newsletters.
5. **International reach** – Over 2600 institutions have access to EPL, enabling your work to be read by your peers in 90 countries.
6. **Open access** – Articles are offered open access for a one-off author payment; green open access on all others with a 12-month embargo.

Details on preparing, submitting and tracking the progress of your manuscript from submission to acceptance are available on the EPL submission website **www.epletters.net**.

If you would like further information about our author service or EPL in general, please visit **www.epljournal.org** or e-mail us at **info@epljournal.org**.

EPL is published in partnership with:

European Physical Society | Società Italiana di Fisica | EDP Sciences | IOP Publishing

A Letters Journal Exploring the Frontiers of Physics

February 2015

EPL, **109** (2015) 47001 www.epljournal.org
doi: 10.1209/0295-5075/109/47001

Dual landscapes in Anderson localization on discrete lattices

M. L. Lyra[1,2], S. Mayboroda[3] and M. Filoche[2,4]

[1] *Instituto de Física, Universidade Federal de Alagoas - 57072-970 Maceió, AL, Brazil*
[2] *Physique de la Matière Condensée, Ecole Polytechnique, CNRS - 91128 Palaiseau, France*
[3] *School of Mathematics, University of Minnesota - Minneapolis, MN, USA*
[4] *CMLA, ENS Cachan, CNRS, UniverSud - Cachan, France*

received 6 January 2015; accepted in final form 4 February 2015
published online 26 February 2015

PACS 71.23.An – Theories and models; localized states
PACS 71.23.-k – Electronic structure of disordered solids
PACS 73.20.Fz – Weak or Anderson localization

Abstract – The localization subregions of stationary waves in continuous disordered media have been recently demonstrated to be governed by a hidden landscape that is the solution of a Dirichlet problem expressed with the wave operator. In this theory, the strength of Anderson localization confinement is determined by this landscape, and continuously decreases as the energy increases. However, this picture has to be changed in discrete lattices in which the eigenmodes close to the edge of the first Brillouin zone are as localized as the low energy ones. Here we show that in a 1D discrete lattice, the localization of low and high energy modes is governed by two different landscapes, the high energy landscape being the solution of a dual Dirichlet problem deduced from the low energy one using the symmetries of the Hamiltonian. We illustrate this feature using the one-dimensional tight-binding Hamiltonian with random on-site potentials as a prototype model. Moreover we show that, besides unveiling the subregions of Anderson localization, these dual landscapes also provide an accurate overall estimate of the localization length over the energy spectrum, especially in the weak-disorder regime.

Introduction. – In Anderson localization [1,2], electronic states are exponentially localized despite the absence of classical confinement, this localization being explained as originating from the destructive interference of waves reflected in the random atomic potential. Despite numerous theoretical advances, such as the prediction by the scaling theory of the lower critical dimension of the Anderson transition [3], there was until recently no general formalism capable to accurately pinpoint the spatial location of these localized modes for any given potential, nor to predict the exact energy at which delocalized modes would begin to form.

Recently, a new theory has been proposed, unveiling in continuous media a direct relationship between any specific realization of the random potential and the corresponding location of localized states [4]. It has been demonstrated that the boundaries of the localization regions, which cannot be deduced by directly looking at the bare random potential, can be accurately retrieved as the valleys lines of a "hidden landscape" $u(\mathbf{x})$ which is the solution of a Dirichlet problem with uniform right-hand side for the same Hamiltonian.

In this article, we show that not only the exact same theory can be extended to the case of a tight-binding Hamiltonian defined on a discrete lattice, but also that, contrary to the continuous case, two different types of localization occur here. First, localization of low energy states can be predicted using a discrete analog of the landscape $u(\mathbf{x})$ defined in the continuous situation. Secondly, the discreteness of the system also triggers a strong localization of states of typical wavelength of the order of the lattice spacing [5–8] (corresponding to the top of the band for a periodic potential). We show that this localization can also be studied in the framework of the landscape theory, with a different operator than the original Hamiltonian and, respectively, a different landscape.

The localization landscape at low energy. – Let us first recall the essential aspects of the theory developed in [4]. In a continuum space, the eigenstates for one particle of mass m in the presence of a potential $V(\mathbf{x})$ are solutions of the time-independent Schrödinger equation

$$[-\Delta + V(\mathbf{x})]\Psi(\mathbf{x}) = E\ \Psi(\mathbf{x}), \tag{1}$$

where units of $\hbar^2/2m$ were considered. The only constraint we impose here on the potential is that it has to be non-negative everywhere: $V(\mathbf{x}) \geq 0$, a condition easily fulfilled by shifting the potential without changing the eigenstates. The new approach allows us to infer several aspects of the eigenstates localization based on a single hidden landscape $u(\mathbf{x})$ which is actually the solution of the corresponding Dirichlet problem

$$[-\Delta + V(\mathbf{x})]u(\mathbf{x}) = 1, \tag{2}$$

with the same boundary conditions as for eq. (1). Every eigenmode (normalized to maximum unitary amplitude) is proved to satisfy the relation

$$|\Psi(\mathbf{x})| \leq Eu(\mathbf{x}) \tag{3}$$

everywhere in the domain. This inequality compels the eigenfunctions to be small at the local minima of $u(\mathbf{x})$ and along the valleys of u considered as a landscape. However, due to the normalization of Ψ in eq. (3), this constraint is only effective in the regions where $u(\mathbf{x}) < 1/E$. Therefore, the portions of the valleys where $u(\mathbf{x})$ is below $1/E$ act as confining borders for the eigenstates, thus defining localization subregions. For higher energies E, the constraint is progressively lifted: neighboring localization subregions merge, up to a point where they form a set that spans the entire domain, signaling the transition to delocalized states. Consequently, while the low energy states are well confined within the valleys of u (*i.e.*, the minima of u in one dimension), higher energy states can permeate through shallow valleys and extend over several neighboring regions. This picture has been mathematically demonstrated and numerically confirmed for several random potentials [9]. Finally, one has to stress here that retrieving the localization landscape requires only solving a Dirichlet problem, a much easier and faster task than computing the entire set of eigenfunctions and eigenvalues of the Hamiltonian (the complexity of the former problem is usually about $N \log N$ where N is the system size, while it is of order $N^2 \log N$ for the latter).

In the following, we consider the quantum mechanical tight-binding problem of one particle restricted to move along a discrete open chain with first-neighbor hopping amplitude t, random on-site potentials V_i, and unitary lattice spacing $a = 1$. For an eigenmode of energy E written as a linear superposition of Wannier local orbitals $|i\rangle$, the components (ψ_i) satisfy the following equation which is the discrete equivalent of the time-independent Schrödinger equation

$$-t[\psi_{i-1} + \psi_{i+1}] + V_i\psi_i = E\psi_i, \tag{4}$$

where $i \in \{1, \ldots, L\}$ denote the chain sites and boundary conditions $\psi_0 = \psi_{L+1} = 0$ are assumed. For an on-site potential ranging from $V_{\min}$ to $V_{\max}$, the spectrum of possible eigenenergies is restricted to the interval $[V_{\min} - 2t, V_{\max} + 2t]$, which implies that the random potential has to be restricted to values $V_i \geq 2t$. Figure 1 displays the two lowest and two highest energy eigenstates

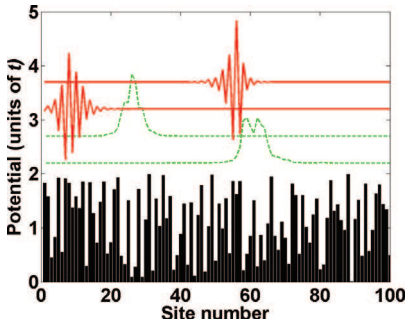

Fig. 1: (Color online) Random potential $V - 2t$ (filled black piecewise constant at the bottom), and the corresponding amplitudes of the two lowest energy states (dashed green lines) and of the two highest energy states (solid red lines). For better visibility, the eigenstates are vertically shifted. The bare potential does not bring a clear indication of where to find to exponentially localized states.

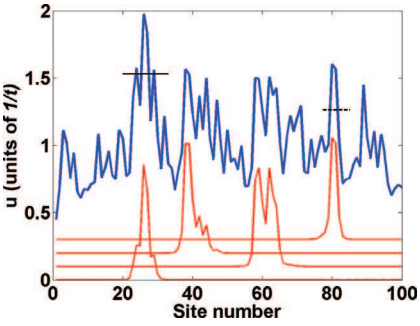

Fig. 2: (Color online) Localization near the bottom of the band: the landscape u_i (top blue line) is plotted together with the probability distribution $|\Psi_i|^2$ of the 4 lowest energy eigenstates (bottom red lines) under the same potential depicted in fig. 1. Two line segments indicate the values of $1/E$ for the fundamental state (left solid line) and for the 4th state (right dashed line). Note that the low energy states are trapped between the minima of u_i which fulfill the confinement condition $u_i < 1/E$.

in a finite chain with $L = 100$ sites for a realization of an i.i.d. random potential uniformly distributed in the interval $[2t, 4t]$. Note that both low and high energy states are exponentially localized but there is no direct indication of where to find their localization region in the original potential. They however differ by an overall phase factor, the low energy states having typically a long wavelength ($k = 2\pi/\lambda \to 0$) while the high energy ones have wavelengths of the order of twice the lattice spacing ($k = 2\pi/\lambda \to \pi/a$).

To unveil the hidden landscape confining the low energy eigenstates, one has to solve the corresponding Dirichlet problem associated to eq. (4) (a rigorous proof of eq. (3) satisfied by the energy eigenfunctions in the discrete case is provided in the appendix):

$$-t(u_{i+1} + u_{i-1} - 2u_i) + (V_i - 2t)u_i = 1, \tag{5}$$

with $u_0 = u_{L+1} = 0$. In fig. 2 we plot the localization landscape u corresponding to the random potential displayed

in fig. 1 together with the probability amplitudes for the 4 lowest energy eigenstates. As predicted by the theory, the profile and location of the lowest energy states are clearly identifiable in the landscape: they are located around the most prominent maxima of u and confined by the deepest minima near each subregion. In the continuous limit where the lattice parameter goes to zero, the above equation resembles a classical Schrödinger equation with uniform right-hand side, and one recovers the localization of quantum states of a continuous Hamiltonian.

The high energy landscape. – Not only the theory of the localization landscape enables us to predict the occurrence of the low energy localized modes, but it also explains the strong localization of high energy states oscillating at a scale close to the lattice parameter (see fig. 3). To this end, one has to examine the behavior of the envelope φ of an eigenmode ψ whose wave vector is close to $k = \pi/a$ (top of the energy band). This envelope is defined by $\psi_i = e^{jkx_i}\varphi_i$, with $x_i = a \times i = i$ being the abscissa of site i. In other words, φ is obtained by removing the fast oscillating contribution to the eigenmode (see the appendix):

$$t\,(\varphi_{i+1} + \varphi_{i-1}) + V_i\varphi_i = E_i\varphi_i. \tag{6}$$

One observes here two symmetry properties of the tight-binding model. First, the symmetry related to a sign change in the hopping amplitude t: this symmetry reverses the energy band. The low (respectively, high) energy states become the high (respectively, low) energy states when reversing the sign of the hopping amplitude: $t \to -t$. Also, they acquire an overall phase of π/a. Reversing the sign of the hopping amplitude is equivalent to reversing the signs of the original random potential and of the corresponding eigenenergies. In order to avoid negative values resulting from this sign change, a global shift V_{shift} has to be applied to the reversed potential, which has again no consequence on the localization properties. The envelope function φ obeys then the following Schrödinger-type equation:

$$-t\,(\varphi_{i+1} + \varphi_{i-1} - 2\varphi_i) + (V_{\text{shift}} - V_i - 2t)\varphi_i = (V_{\text{shift}} - E_i)\varphi_i. \tag{7}$$

Therefore, the appropriate dual Dirichlet problem that provides the confinement landscape for the high energy states takes the form

$$-t(u^*_{i+1} + u^*_{i-1} - 2u^*_i) + (V_{\text{shift}} - V_i - 2t)u^*_i = 1, \tag{8}$$

where V_{shift} is a constant chosen such that $V_{\text{shift}} - V_i - 2t \geq 0$ everywhere. To keep the potential in the dual Dirichlet problem in the same range as the one in the original Dirichlet problem, the global shift has to be $V_{\text{shift}} = V_{\min} + V_{\max}$.

In fig. 3 we show the resulting dual landscape (top curve) for the same random potential displayed in fig. 1, together with the 4 highest energy states. Although these states present spatial oscillations at the scale of the lattice parameter, the dual landscape u^* clearly signals the subregions of localization close to its most prominent maxima. Also, the confinement strength decreases as one departs from the top of the band, the confinement condition at $u_i < 1/E$ being replaced by $u^*_i < 1/(V_{\text{shift}} - E)$.

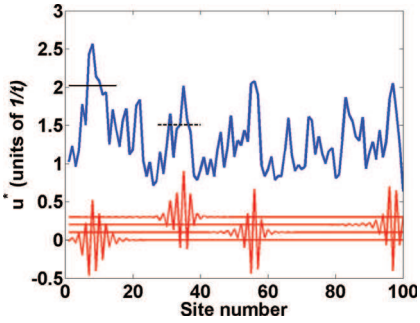

Fig. 3: (Color online) Localization near the top of the band: the dual landscape u^* is plotted together with the 4 eigenstates of highest energy corresponding to the same potential as depicted in fig. 1. Two line segments indicate the values of $1/(V_{\text{shift}} - E)$ for the highest energy state (solid line) and for the 4th state from the top of the band (dashed line). Here, $V_{\text{shift}} = 6t$. The high energy states are localized in subregions of u^* close to its most prominent peaks, and are confined between the minima of u^* that fulfill the confining condition $u^* < 1/(6t - E)$.

We now show that these landscapes u and u^* can allow us to compute an estimate of the average localization length of the eigenstates around any given energy. This estimate will then be compared to the participation ratio of each mode ψ, a widely used measurement of the localization length [10,11], defined as

$$P = \left(\sum_i |\psi_i|^2\right)^2 \Big/ \left(\sum_i |\psi_i|^4\right). \tag{9}$$

This ratio is usually understood as a measure of the number of sites on which the particle probability distribution is concentrated. It is of the order of the localization length for exponentially localized states while for a uniform potential, all harmonic eigenstates have an identical participation ratio equal to $2L/3$, L being the chain length.

To pinpoint the confining sub-region —defined by the landscape u— associated with an eigenstate of low energy E_k, we first locate the chain site $i_{\max}$ at which this specific state has its largest amplitude. We then define the size of the localization subregion ξ_k as the length $(j-i)a$ of the smallest interval $[i, j]$ containing $i_{\max}$ (*i.e.* $i < i_{\max} < j$) such that u_i and u_j are local minima of u that are both smaller than $1/E_k$. In other words, i and j are the nearest "valleys" of the landscape u surrounding this eigenstate. For high energy modes, a similar procedure is employed using the dual landscape u^* and $1/(V_{\text{shift}} - E)$ as the confinement strength criterion.

In fig. 4 we evidence the very strong correlation between the participation ratio P_k and the size of the confining subregions ξ_k by plotting the histogram of the

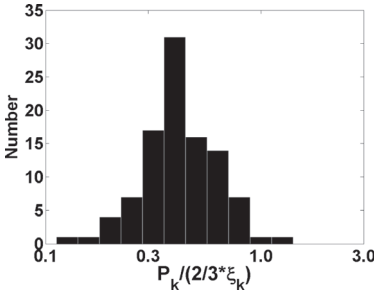

Fig. 4: Histogram in log scale of the ratio $P_k/(2/3\xi_k)$ for the bottom 50 and top 50 eigenstates in a chain of $L = 200$ sites and a random potential V whose values range in the interval $[2t; 10t]$ (see eq. (9) and the following text for the definitions of P_k and ξ_k). This histogram shows that both quantities are always of the same order for localized eigenstates.

ratio $P_k/(2/3\xi_k)$ for the 50 states of lowest energy and the 50 states of highest energy in a chain of length $L = 200$ (*i.e.*, half of the states, their total number being 200). Note that $P_k/(2/3\xi_k)$ can take in theory any value ranging from $1/(2/3L)$ to $L/(4/3)$. Although the participation ratio of an individual eigenstate may vary from a few sites to the entire length of the chain, both quantities appear to be always of the same order of magnitude.

This strong correlation provides a key to introducing an even simpler estimate of the localization length, called here $\delta(E)$ which depends only on the energy value E. It is obtained by averaging all distances between minima of u which are below $1/E$, and then multiplying the obtained quantity by 2/3. Therefore $\delta(E)$ can be understood as averaging the sizes ξ of all subregions found below $1/E$, independently of their location in the system and thus be used as a rough estimate of the average localization length of all eigenmodes of energy around E.

In fig. 5, we superimpose plots of the participation ratio for each eigenstate (circles) and the average size $\delta(E)$ of the localization subregions (line). For the bottom half of the spectrum, $\delta(E)$ is computed using the landscape u, whereas the dual landscape u^* is used for the upper half. Two representative cases of disorder, weak and strong (fig. 5, respectively left and right), are illustrated. In the case of weak disorder, $\delta(E)$ reproduces the behavior of the average participation ratio over the entire energy band, correctly predicting the location of the pseudo-mobility edges separating the well-localized from the delocalized states. These delocalized states have an harmonic-like form with random phase changes. Consequently, their participation ratios fluctuate around $2L/3$. Accordingly, $\delta(E)$ reaches a plateau at $2L/3$ in the energy range corresponding to effectively delocalized states signaling that the dual landscapes have no minima below the threshold level in this energy range.

In the regime of strong disorder all states become well localized with no pseudo-mobility edges within the band of allowed energies. The average size $\delta(E)$ also captures such strong localization, although near the center of the band it

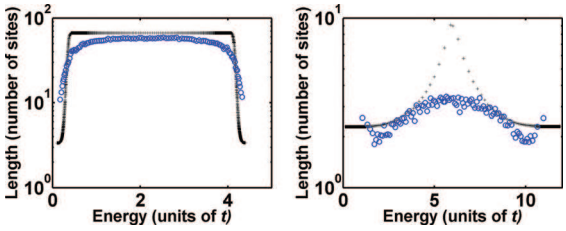

Fig. 5: (Color online) Participation ratio (circles) and $\delta(E)$ (crosses), the latter corresponding to 2/3× the average size of the confining subregions for eigenfunctions of energy smaller than E (see below). In order to reduce the stochastic fluctuations, both quantites have been averaged over 100 realizations of the random potential. Left panel: weak-disorder regime ($V = [2t; 2.5t]$). Notice that the average size of the confining subregions closely follows the main trends of the participation number in the whole energy spectrum; right panel: strong-disorder regime ($V = [2t; 10t]$). The length $\delta(E)$ computed using the two potentials u and u^* capture the strong localization of the eigenstates.

signals a weaker localization, a fact already well known in the literature [12]. This behavior reflects the fact that the continuous Laplacian operator does not properly describe all features of the discrete tight-binding Hamiltonian near the band center.

One can compare our approach to the semi-classical picture by assessing the value of the parameter η classically defined as the ratio V_0/E_0 between the typical depth of the wells created by the random potential and the typical fundamental energy of a quantum particle in a well [13]. In our case, the correlation length of the random potential is the lattice parameter ($a = 1$). With our unit choice, this gives $E_0 = \hbar^2/(2ma^2) = 1$. Therefore the parameter η corresponds to the potential amplitude $(V_{\max} - V_{\min})$ in our discrete model. In the regime of strong disorder (large η, fig. 5, right) all states are well localized. In the first half of the energy band they localize around minima of the potential and in the second half around maxima. In this regime of strong disorder, our localization landscape is quite rough with minima and maxima following closely the respective maxima and minima of the original potential. This is fully consistent with the semi-classical approach. In the weak-disorder regime (fig. 5, left), the states become less localized, and the particle does not experience the detail of the disordered potential but a smoothed effective potential. Our approach allows determining exactly the energy range and the location of the localized states. The scheme of delocalization arising from the merging of subregions provides a new interpretation of the effective delocalization transition taking place in finite chains with weak disorder.

Conclusions. – In summary, we have shown here that the localization of one-particle eigenstates satisfying a discrete time-independent Schrödinger equation is in reality governed by a pair of dual landscapes, u and u^*, *a priori* invisible to the naked eye, respectively acting on the

regimes of low and high energies. We demonstrated that the appropriate Dirichlet problem whose solution unveils the landscape of localization has distinct forms near the bottom and the top of the energy band. Using the symmetries of the tight-binding Hamiltonian, the landscape confining the high energy states is found to be the solution of an alternate Dirichlet problem with a new potential. Although a full geometrical interpretation of Anderson localization has yet to be found, these dual landscapes signal the localization subregions in both energy regimes, a task that had not been successfully achieved in prior studies aiming to provide a geometrical analysis for this phenomenon.

The distinct confinement strengths of the hidden landscapes were used to introduce a new measure of the localization length. We showed that, despite its approximate nature, the average size of the confining subregions $\delta(E)$ captures well the main dependence of the localization length within the range of allowed energies, especially in the regime of weak disorder at which $\delta(E)$ clearly signals the location of the pseudo-mobility edges separating well-localized from effectively delocalized states.

The present scenario opens a totally new perspective to the geometric interpretation of Anderson localization in discrete lattices based on the hidden landscapes u and u^*. Specifically, in 2 or 3 dimensions, one can extrapolate that u will remain as the low energy landscape while u^* has to be replaced by a collection of landscapes, each corresponding to one boundary of the first Brillouin zone of the lattice. This approach also raises a number of new questions that remain to be addressed. Could it be possible to unify the present description based on several distinct landscapes into a wave-vector–dependent landscape scenario valid for the whole energy band? Can these landscapes signal resonant delocalized states that are usually depicted by discrete tight-binding models with correlated disorder [14–17] or inter-particle interactions [18–22]? In this context, it would be very interesting to assess how these interactions can distort the landscapes. New analytical and numerical efforts along these directions will certainly contribute to unveil a new geometrical picture of the Anderson localization in all discrete lattices.

* * *

This work was partially funded by the Brazilian Research Agencies CAPES, CNPq, FINEP and FAPEAL. The sabbatical stay of MLL at Physique de la Matière Condensée Lab was funded through the Grant ATLAS from the Triangle de la Physique. MF is partially supported by a PEPS-PTI Grant from CNRS. SM is partially supported by the Alfred P. Sloan Fellowship, the NSF CAREER Award DMS 1056004, the NSF MRSEC Seed Grant, and the NSF INSPIRE Grant.

Appendix: control inequality for a discrete Schrödinger operator. – We present here the mathematical proofs of the main inequalities, in particular eq. (3), controlling the wave function in the discrete case. The arguments are fairly straightforward, but it is important that they are proved directly in the discrete scenario (rather than appealing to approximation by a continuous model).

Let us denote by Δ_D the discrete Laplacian, that is, for $u := (u_1, \ldots, u_L)^\perp$ (colon vector) we write

$$(\Delta_D u)_i := u_{i+1} + u_{i-1} - 2u_i. \tag{10}$$

Given a potential V_i defined at each site, we consider the Schrödinger-type operator $-t\Delta_D + W$ such that

$$\begin{aligned}(-t\Delta_D + Wu)_i &:= -t(u_{i+1} + u_{i-1} - 2u_i) + (V_i - 2t)u_i \\ &= -t(u_{i+1} + u_{i-1} - 2u_i) + W_i u_i, \end{aligned} \tag{11}$$

where $t > 0$ and $W = (W_1, \ldots, W_L)^\perp$ is such that $V_i \geq 2t$ for all i and hence, $W_i \geq 0$ for all i. Clearly, the operator $-t\Delta_D + W$ can be identified with multiplication from the left by a matrix A with values $A_{ii} = 2t + W_i$, $i = 1, \ldots, L$, on the main diagonal, $W_{i,i-1} = -t$, $i = 2, \ldots, L$, $W_{i+1,i} = -t$, $i = 1, \ldots, L-1$ on lower and upper diagonal, and 0 otherwise.

Lemma 1. (Maximum principle). *Let $t > 0$ and $W \geq 0$ as above. If $((-t\Delta_D + W)u)_i \geq 0$, $i = 1, \ldots, L$, and $u(0) = u(L+1) = 0$, then $u_i \geq 0$ for all $i = 1, \ldots, L$. Moreover, if there exists an i_0 such that $((-t\Delta_D + W)u)_{i_0} > 0$ then $u_i > 0$ for all $i = 1, \ldots, L$.*

Proof. We prove by contradiction. Let us assume that there is a minimum "inside" the domain, that is, there exists i_0 such that $u_{i_0} \leq u_{i_0+1}$ and $u_{i_0} \leq u_{i_0-1}$. Then $u_{i+1} + u_{i-1} - 2u_i \geq 0$. But $((-t\Delta_D + W)u)_i \geq 0$, hence, $t(u_{i+1} + u_{i-1} - 2u_i) \leq W_i u_i$. Hence, $u_i \geq 0$, but we assumed that it was a minimum and hence, that it was below the boundary values equal to zero. This is a contradiction. We conclude that the minimum could not be "inside" the domain and hence, that all interior values of u are non-negative.

In order to show strict positivity, it is enough to demonstrate that if $u_{i_0} = 0$ at some i_0, then $((-t\Delta_D + W)u)_i = 0$ for all i. To this end, let us assume that $u_{i_0} = 0$ at some $1 \leq i_0 \leq L$. Since it cannot be a local minimum, the values of u_{i_0-1}, u_{i_0+1} must be smaller or equal than $u_{i_0} = 0$. Since they cannot be below zero, we have $u_{i_0-1}, u_{i_0+1} = 0$. Continuing in this fashion, we conclude that $u_0 \equiv 0$ and hence, $((-t\Delta_D + W)u)_i = 0$ for all i, as desired. □

Lemma 2. (Positivity). *For the matrix A associated with the operator $-t\Delta_D + W$ as above, the inverse exists and every entry of the inverse is strictly positive.*

This is an analogue of the positivity of the Green function.

Proof. Let $((-t\Delta_D + W)u)_i = f_i$, $i = 1, \ldots, L$, $u_0 = u_{L+1} = 0$. In matrix notation, $A\vec{u} = \vec{f}$. Then $u_j = (A^{-1}f)_j = \sum_{k=1}^{L} (A^{-1})_{jk} f_k$. If we take $\vec{f}$ as a vector

with 0 entries except for 1 in the l-th place, then $u_j = (A^{-1})_{jl}$. By (the second statement of) Lemma 1, all u_j, $j = 1, \ldots, L$ must be strictly positive, as desired. □

Lemma 3. (Inequality (3) in the discrete case). *Let*

$$((-t\Delta_D+W)\psi)_j = \lambda\psi_j, \quad j = 1, \ldots, L, \quad \psi_0 = \psi_{L+1} = 0,$$

where the operator is defined as in (11) *with* $t > 0$ *and it is assumed that* $W = V - 2t \geq 0$. *Then*

$$\frac{|\psi_j|}{\max_k |\psi_k|} \leq \lambda u_j, \quad \textit{for all } j = 1, \ldots, L,$$

where u *solves*

$$((-t\Delta_D + W)u)_j = 1, \quad j = 1, \ldots, L, \quad u_0 = u_{L+1} = 0.$$

Proof. This is a simple consequence of the Lemmas above. Indeed, using the positivity established in Lemma 2,

$$\begin{aligned}\psi_j = (\lambda A^{-1}\psi)_j = \lambda \sum_{k=1}^{L} (A^{-1})_{jk}\psi_k \leq \lambda \max_k |\psi_k| \sum_{k=1}^{L} (A^{-1})_{jk} \\ = \lambda \max_k |\psi_k| u_j.\end{aligned}$$

□

Lemma 3, applied, as above, with $W = V - 2t$, furnishes inequality (3) in the main manuscript of the paper for the discrete model, and respectively, treats the lower-energy modes. To address the higher-order ones, we apply the transform $\psi_j = e^{i\alpha j}\varphi_j$, $j = 1, \ldots, L$, $\alpha \in \mathbb{R}$. Note the change of notation: from now on, i is the imaginary unit. Then the eigenfunctions of $(-t\Delta_D+W) = (-t\Delta_D+V-2t)$ as above, denoted by ψ, are transformed into the "envelope" functions φ satisfying the following equation:

$$-t(e^{i\alpha}\varphi_{j+1} + e^{-i\alpha}\varphi_{j-1}) + V_j\varphi_j = \lambda\varphi_j.$$

The choice $\alpha = \pi$, optimal for studying the eigenfunctions at the high end of the band gap, yields

$$t(\varphi_{j+1} + \varphi_{j-1}) + V_j\varphi_j = \lambda\varphi_j,$$

or, as discussed in the paper,

$$-t(\varphi_{j+1}+\varphi_{j-1}-2\varphi_j)+(V_{\text{shift}}-2t-V_j)\varphi_j = (V_{\text{shift}}-\lambda)\varphi_j,$$

where V_{shift} is chosen to ensure that $V_{\text{shift}} - 2t - V_j \geq 0$.

Zero Dirichlet boundary conditions on ψ trivially yield zero Dirichlet boundary conditions for φ, and hence, Lemma 3 yields the following corollary.

Corollary 4. (Inequality (3) for the dual landscape). *Let*

$$((-t\Delta_D+W)\psi)_j = \lambda\psi_j, \quad j = 1, \ldots, L, \quad \psi_0 = \psi_{L+1} = 0,$$

where the operator is defined as in (11) *with* $t > 0$. *Let furthermore* φ_j *denote the envelopes of* ψ_j, *defined via* $\psi_j = e^{i\alpha j}\varphi_j$, $j = 1, \ldots, L$. *Then for any choice of* V_{shift} *such that* $V_{\text{shift}} - 2t - V \geq 0$, *we have*

$$\frac{|\varphi_i|}{\max_j |\varphi_j|} \leq (V_{\text{shift}} - \lambda)u_i^*, \quad \textit{for all} \quad i = 1, \ldots, L,$$

where u *solves*

$$((-t\Delta_D + W^*)u^*)_i = 1, \quad i = 1, \ldots, L, \quad u_0 = u_{L+1} = 0,$$

with $W^* = V_{\text{shift}} - 2t - V \geq 0$.

REFERENCES

[1] Anderson P. W., *Phys. Rev.*, **109** (1958) 1492.
[2] Lagendijk A., van Tiggelen B. and Wiersma D. S., *Phys. Today*, **62**, issue No. 8 (2009) 24.
[3] Abrahams E., Anderson P. W., Licciardello D. C. and Ramakrishnan T. V., *Phys. Rev. Lett.*, **42** (1979) 673.
[4] Filoche M. and Mayboroda S., *Proc. Natl. Acad. Sci. U.S.A.*, **109** (2012) 14761.
[5] John S., *Phys. Rev. Lett.*, **58** (1987) 2486.
[6] Desideri J.-P. and Sornette D., *Europhys. Lett.*, **23** (1993) 165.
[7] Quang T., Woldeyohannes M., John S. and Agarwal G. S., *Phys. Rev. Lett.*, **79** (1997) 5238.
[8] Deych L. I., Erementchouk M. V., Lisyansky A. A. and Altshuler B. L., *Phys. Rev. Lett.*, **91** (2003) 096601.
[9] Filoche M. and Mayboroda S., *Contemp. Math.*, **601** (2013) 113.
[10] Thouless D., *Phys. Rep.*, **13** (1974) 93.
[11] Prelovsek P., *Phys. Rev. Lett.*, **40** (1978) 1596.
[12] Deych L. I., Lisyansky A. A. and Altshuler B. L., *Phys. Rev. Lett.*, **84** (2000) 2678.
[13] Shapiro B., *J. Phys. A: Math. Theor.*, **45** (2012) 143001.
[14] Dunlap D. H., Wu H. L. and Phillips P. W., *Phys. Rev. Lett.*, **65** (1990) 88.
[15] Wu H. L. and Phillips P., *Phys. Rev. Lett.*, **66** (1991) 1366.
[16] Hilke M., *J. Phys. A*, **30** (1997) L367.
[17] de Moura F. A. B. F., Coutinho M. D., Lyra M. L. and Raposo E. P., *Europhys. Lett.*, **66** (2004) 585.
[18] Srinivasan B., Benenti G. and Shepelyansky D. L., *Phys. Rev. B*, **67** (2003) 205112.
[19] Dias W. S., Nascimento E. M., Lyra M. L. and de Moura F. A. B. F., *Phys. Rev. B*, **76** (2007) 155124.
[20] Song Y., Wortis R. and Atkinson W. A., *Phys. Rev. B*, **77** (2008) 054202.
[21] Henseler P., Kroha J. and Shapiro B., *Phys. Rev. B*, **77** (2008) 075101.
[22] DeLuca A., Altshuler B. L., Kravtsov V. E. and Scardicchio A., *Phys. Rev. Lett.*, **113** (2014) 046806.